10.21062/mft.2020.119 http://www.journalmt.com

Research on Optimization of a High Precision Hydrostatic Turntable

Lai Hu, Yaolong Chen
School of Mechanical Engineering, Xi'an Jiaotong University, 28 Xianning Road, Xi'an, Shaanxi 710049, P.R. China. E-mail: chenzwei@mail.xjtu.edu.cn (Yaolong Chen)

This paper mainly studies the hydrostatic turntable of precision milling and grinding compound machining center in aerospace processing equipment, and innovatively designs and analyzes the mesa. It is proposed to replace the traditional 40Cr with imported marble for the mesa. Firstly, the vibration model of the hydrostatic turntable is carried out. ANSYS Workbench software is used to compare and analyze the original and marble materials. In the process, the static characteristics and the difference of first-order modes of the two materials are compared. In addition, the analytical results are used for manufacturing. The results show when the applied force reaches the limitation 29400N, the maximum displacement of 40Cr increases sharply to 8.9406μm; while the marble material reaches 2.6μm. Meanwhile, it is obtained that the power consumed by marble is reduced by 39.12% compared with 40Cr. The weight of marble is reduced by 39.36% compared with 40Cr. Marble is about 21.59% higher than 40Cr in the comparison of vibration mode results.

Keywords: Milling and grinding compound machining center, Hydrostatic turntable, Innovative design, Compared, Marble

1 Introduction

The development of aerospace technology always represents one of the factors of a country's military strength. Generally speaking, aerospace technology belongs to high precision equipment. However, there are many aspects of traditional research on high-precision equipment, and many scholars have also carried out research. For example, Brecher C et al. [1] followed a compact design strategy and developed two high-precision machine tools by reducing the overall size of the machine. The development of two kinds of compact machine tools shows that the compact design improves the dynamic performance and accuracy. Chen E P et al. [2] designed a double-axis rotary milling head with large torque, high precision and high rigidity with an output torque of 3000Nm. Therefore, a new design scheme of double-axis rotary milling head with mechanical spindle, gear transmission and swing fork structure is proposed. The contradiction between large reduction ratio and high precision transmission is solved. Chen W et al. [3] introduced an integrated system for the conceptual design and basic design stages of ultra-precision machine tools. This system is based on dynamics, thermodynamics and error budget theory. Liang, Y.C [4] proposed a dynamic design method for ultra-precision machine tools based on the requirements of workpiece morphology. Starting from the morphological characteristics and functional requirements of the workpiece, this method demonstrates how to design and analyze the kinematic chain and configuration of the machine tool. Chen G D et al. [5] proposed a dynamic precision design method for ultra-precision machine tools based on frequency domain error allocation. The feasibility of the proposed DAD method is illustrated by an example.

Of course, there are also scholars who have studied the hydrostatic turntable in aerospace processing equipment. For example, Zhao Y.S et al. [6] developed a simulation model to analyze the influence of guide rail profile error on the motion accuracy of hydrostatic turntable. According to Reynolds equation of lubricating film, the reaction forces of preloaded thrust bearing and hydrostatic circular oil pad are obtained. The motion equation of static pressure turntable considering the contour error of the two guide rails is derived. The results show that wavelength, profile error amplitude, velocity amplitude and turntable offset load can all affect the motion accuracy of hydrostatic turntable. Zhaomiao L et al. [7] studied the numerical simulation of the flow, bearing and carrying capacity of cycloidal hydrostatic oil chamber under the rotating speed of 0~5 m/s and different boundary conditions. IWASAKI, Makoto et al. [8] proposed a new research method of high precision contour control for machine tool worktable transmission system. The proposed method has significant performance improvement in accurate table contour control. Adong Y U et al. [9] developed a rotary worktable to improve the accuracy retention of large-scale high-precision vertical numerical control machine tools. The turntable adopts a set of radial thrust tapered roller bearings, eliminating the

traditional spindle and complex spindle bearing system. The bottom ring and the top ring of the radial thrust tapered roller bearing are installed on the same shaft table, which eliminates the clearance between each bearing ring and its components, realizes interference fit, and greatly improves the accuracy retention of the machine tools. In addition, the author has also studied the other related components of the turntable, the purpose of which is also to improve the rotation accuracy of the turntable. In view of the above authors' research, this paper proposes an innovative design of the turntable system. In the mesa optimization, imported marble material are mainly used to replace the traditional 40Cr. Because the anti-vibration strength and stability of marble are higher than 40Cr. And with the increase of the service life of the machine tools, the overall accuracy maintenance ability of the machine tools will not be changed basically. In this paper, the theoretical vibration model of turntable components is deduced at first. Secondly, the advantages and disadvantages of marble and 40Cr are further explained by means of analysis and comparison. Finally, processing and production are carried out through the analysis results, and quantitative conclusions are drawn.

2 Theoretical analysis

Before analyzing 40Cr and marble mesa, theoretical analysis of mesa vibration system is needed. Firstly, the quality of the turntable top system is simplified, as shown in Fig. 1.

As shown in Fig. 1, the diagram of the vibration system consists of three parts: 40Cr table top, marble turntable and fastening screw. The surface of the worktable bears gravity, and the lower surface of the worktable is in a fixed mode and rotates around the Y axis.

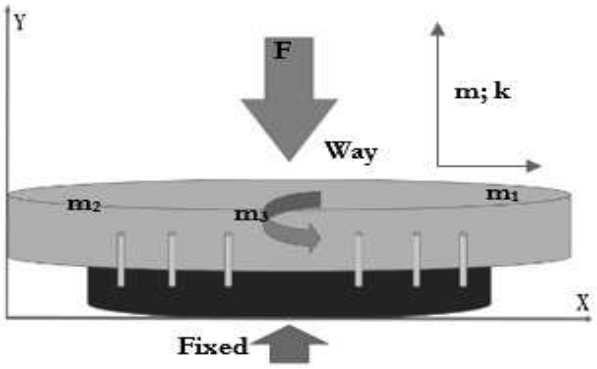

Fig. 1 *Simplified diagram of turntable surface vibration system.*

Therefore, the vibration dynamics analysis Eq. [10-11] is:

$$[K]\{X\}+[C]\{\dot{X}\}+[M]\{\ddot{X}\}=\{F(t)\} \tag{1}$$

Considering undamped structure, partial constraints and external load factors, the Eq. (1) can be expressed as:

$$[M]\{\ddot{X}\}+[K]\{X\}=\{29400\} \tag{2}$$

Of which, $\{F(t)\}$ is the external load; $[K]$ is the stiffness matrix; $[C]$ is the damping matrix; $\{X\}$、$\{\dot{X}\}$、$\{\ddot{X}\}$ is the set of displacements of each node, its first derivative and second derivative respectively, and is also the modal shape; $[M]$ is the mass matrix.

In this research system, the mass matrix includes the mass and inertia parameters of the powertrain, which are expressed as follows:

$$M=\begin{bmatrix} m_1 & 0 & 0 & 0 & 0 & 0 \\ 0 & m_2 & 0 & 0 & 0 & 0 \\ 0 & 0 & m_3 & 0 & 0 & 0 \\ 0 & 0 & 0 & I_{xx} & -I_{xy} & -I_{zx} \\ 0 & 0 & 0 & -I_{xy} & I_{yy} & -I_{yz} \\ 0 & 0 & 0 & -I_{zx} & -I_{yz} & I_{zz} \end{bmatrix} \tag{3}$$

However, through the derivation of Eq. (2), it is concluded that:

$$\begin{bmatrix} k_1+k_2 & -k_2 & 0 & 0 & 0 & 0 \\ -k_2 & k_2+k_3 & -k_3 & 0 & 0 & 0 \\ 0 & -k_3 & k_3+k_4 & -k_4 & 0 & 0 \\ 0 & 0 & -k_4 & k_4+k_5 & -k_5 & 0 \\ 0 & 0 & 0 & -k_5 & k_5+k_6 & -k_6 \\ 0 & 0 & 0 & 0 & -k_6 & k_6 \end{bmatrix} \begin{Bmatrix} x_1 \\ x_2 \\ x_3 \\ x_4 \\ x_5 \\ x_6 \end{Bmatrix} + \begin{bmatrix} m_1 & 0 & 0 & 0 & 0 & 0 \\ 0 & m_2 & 0 & 0 & 0 & 0 \\ 0 & 0 & m_3 & 0 & 0 & 0 \\ 0 & 0 & 0 & I_{xx} & -I_{xy} & -I_{zx} \\ 0 & 0 & 0 & -I_{xy} & I_{yy} & -I_{yz} \\ 0 & 0 & 0 & -I_{zx} & -I_{yz} & I_{zz} \end{bmatrix} \begin{Bmatrix} \ddot{x}_1 \\ \ddot{x}_2 \\ \ddot{x}_3 \\ \ddot{x}_4 \\ \ddot{x}_5 \\ \ddot{x}_6 \end{Bmatrix} = \{29400\} \tag{4}$$

In Eq. (4), consider that the inertia product I_{xx}、I_{yy}、I_{zz} is expressed by I :

$$I=\begin{bmatrix} I_{xx} & I_{xy} & I_{zx} \\ I_{xy} & I_{yy} & I_{yz} \\ I_{zx} & I_{yz} & I_{zz} \end{bmatrix} \tag{5}$$

The Eq. (5) also represents an inertial matrix composed of a rigid body for a spatial coordinate system Oxyz.

Among them, the table top and worktable of this turntable are symmetrical models. Therefore, diagonal elements are moments of inertia, defined as:

$$I_{xx} = \iiint \left(y^2 + z^2\right) dm \tag{6}$$

$$I_{yy} = \iiint \left(x^2 + z^2\right) dm \tag{7}$$

$$I_{zz} = \iiint \left(x^2 + y^2\right) dm \tag{8}$$

Combining the calculation Eqs. (6-8) of space inertia parameters and triple integral, the following results are obtained:

$$\begin{cases} I_{xx} = \iiint \left(y^2 + z^2\right) dm = \iiint \left(y^2 + z^2\right) \rho dV = \dfrac{1}{12} \rho abc\left(b^2 + c^2\right) \\ I_{yy} = \iiint \left(x^2 + z^2\right) dm = \iiint \left(x^2 + z^2\right) \rho dV = \dfrac{1}{12} \rho abc\left(a^2 + c^2\right) \\ I_{zz} = \iiint \left(x^2 + y^2\right) dm = \iiint \left(y^2 + x^2\right) \rho dV = \dfrac{1}{12} \rho abc\left(b^2 + a^2\right) \end{cases} \tag{9}$$

Further analysis shows that:

$$\begin{cases} a = \sqrt{\dfrac{6\left(-I_{xx} + I_{yy} + I_{zz}\right)}{m_{move}}} \\ b = \sqrt{\dfrac{6\left(I_{xx} - I_{yy} + I_{zz}\right)}{m_{move}}} \\ c = \sqrt{\dfrac{6\left(I_{xx} + I_{yy} - I_{zz}\right)}{m_{move}}} \\ \rho = \dfrac{m_{move}}{abc} \end{cases} \tag{10}$$

Therefore, the size a、b、c and density ϱ of the inertial body are derived by combining the inertia product I_{xx}、I_{yy}、I_{zz} and the powertrain mass m_{move}.

At the same time, combined with Eqs. (4) and (9) and deduced, the following results are obtained:

$$\begin{bmatrix} k_1 + k_2 & -k_2 & 0 & 0 & 0 & 0 \\ -k_2 & k_2 + k_3 & -k_3 & 0 & 0 & 0 \\ 0 & -k_3 & k_3 + k_4 & -k_4 & 0 & 0 \\ 0 & 0 & -k_4 & k_4 + k_5 & -k_5 & 0 \\ 0 & 0 & 0 & -k_5 & k_5 + k_6 & -k_6 \\ 0 & 0 & 0 & 0 & -k_6 & k_6 \end{bmatrix} \begin{Bmatrix} x_1 \\ x_2 \\ x_3 \\ x_4 \\ x_5 \\ x_6 \end{Bmatrix} + \begin{bmatrix} m_1 & 0 & 0 & 0 & 0 & 0 \\ 0 & m_2 & 0 & 0 & 0 & 0 \\ 0 & 0 & m_3 & 0 & 0 & 0 \\ 0 & 0 & 0 & \frac{1}{12}\rho abc\left(b^2 + c^2\right) & -I_{xy} & -I_{zx} \\ 0 & 0 & 0 & -I_{xy} & \frac{1}{12}\rho abc\left(a^2 + c^2\right) & -I_{yz} \\ 0 & 0 & 0 & -I_{zx} & -I_{yz} & \frac{1}{12}\rho abc\left(b^2 + a^2\right) \end{bmatrix} \begin{Bmatrix} \ddot{x}_1 \\ \ddot{x}_2 \\ \ddot{x}_3 \\ \ddot{x}_4 \\ \ddot{x}_5 \\ \ddot{x}_6 \end{Bmatrix} = \{29400\} \tag{11}$$

Finally, the first six modal functions of the simplified turntable system will be analyzed and expressed by $\left\{A^{(1)}\right\}$、$\left\{A^{(2)}\right\}$、$\left\{A^{(3)}\right\}$、$\left\{A^{(4)}\right\}$、$\left\{A^{(5)}\right\}$、$\left\{A^{(6)}\right\}$.

3 Simulation analysis of vibration and statics of different materials

In order to better analyze the excellence of marble and 40Cr, it is necessary to apply the two materials to the turntable components and study them respectively. At the same time, before vibration and statics simulation analysis, the overall structure of the turntable needs to be analyzed, as shown in Fig. 2.

In the research of traditional high-precision machine tools hydrostatic turntable, the marble turntable in Fig. 2 uses 40Cr material. According to Fig. 2, the vibration mode and statics analysis of the combination of 40Cr mesa and marble turntable will be separately carried out. Firstly, the model is imported into the analysis software ANSYS Workbench and generated mesh [12-13]. At that same time, marble and 40Cr were applied to the marble turntable of Fig. 2, respectively. The two material parameter pairs are shown in Tab. 1.

Tab. 1 *Comparison of marble and 40Cr parameters.*

Materials / Parameters	Marble	40Cr
Density	3.09g/cm3	7.9 g/cm3
Young's modulus	50GPa	209000GP
Average linear expansion coefficient	7.36 10-6°C-1	11.9 10-6°C-1
Poisson's ratio	0.3	0.277
Compressive strength	366MPa	365.7MPa
Weight	172.003Kg	436.96555Kg
Water absorption	0.026%	
Hardness	505HB	207HB

Fig. 2 *Three-dimensional model of hydrostatic turntable.*

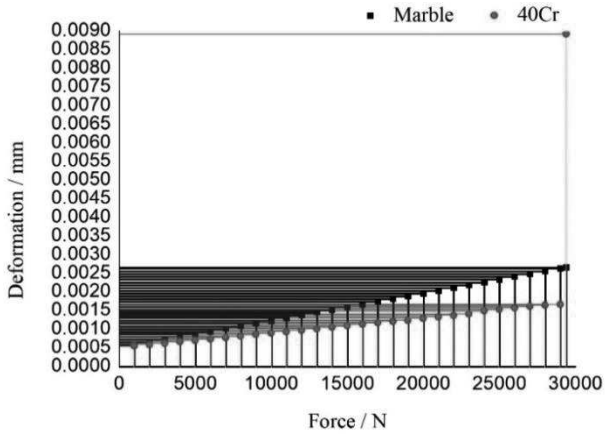

Fig. 3 *Analysis and comparison of marble and 40Cr (1000N-29400N).*

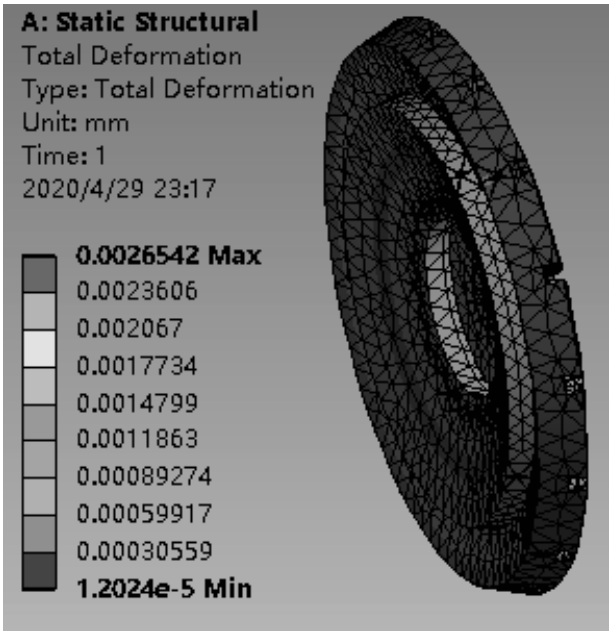

Fig. 4 *Maximum displacement of marble (29400N).*

As shown in Figs. 1 and 2, a boundary condition is applied. The lower surface of the marble turntable is set as a fixed constraint, while only rotating around the Y axis is reserved, and the rest displacements are set to 0 mm. A limit force of 29400N is applied to surface of the 40Cr mesa shown in Fig. 2 in a direction from top to bottom and a maximum rotational speed of 10.47 rad/s was applied too. After the setting is completed, force (1000N-29400N) is applied to marble and 40Cr respectively and maximum displacement analysis is carried out, as shown in Fig. 3. Meanwhile, the simulated results of marble and 40Cr at 29400N are presented separately. As shown in Figs. 4-6 and Figs. 7-9, respectively.

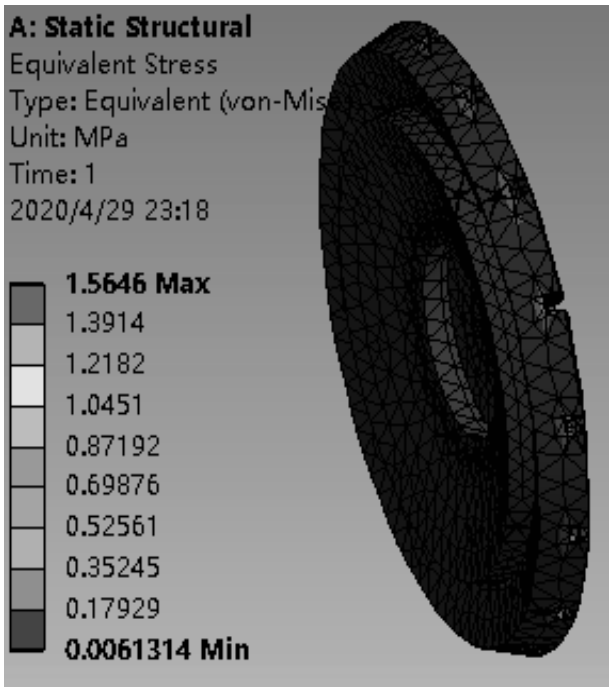

Fig. 5 *Maximum stress of marble (29400N).*

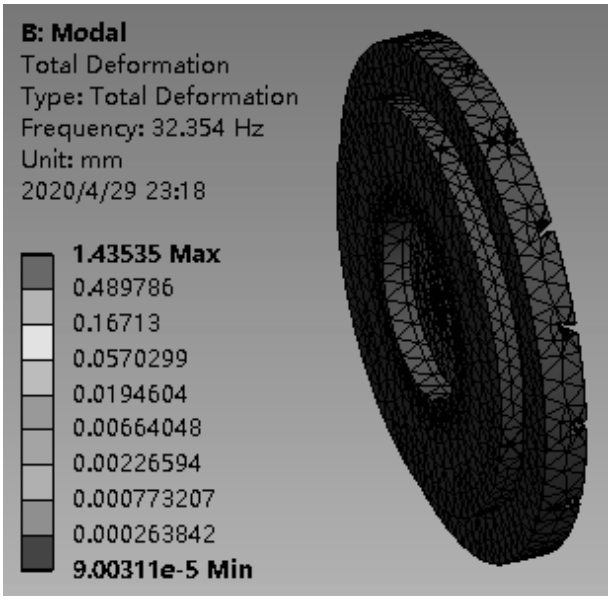

a) First-order mode

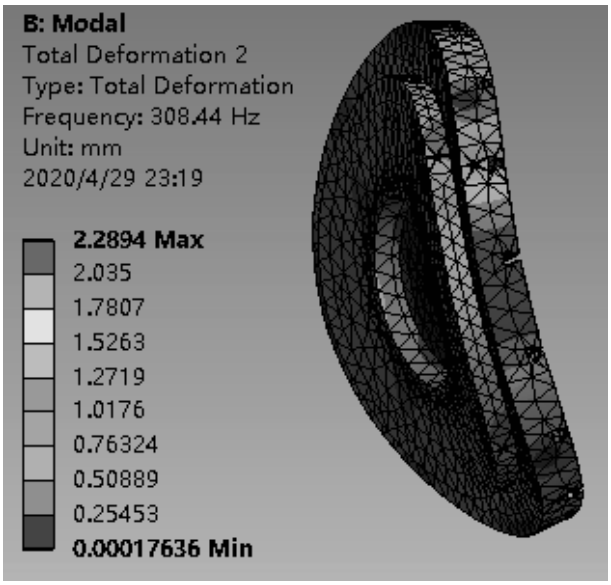

b) Second-order mode

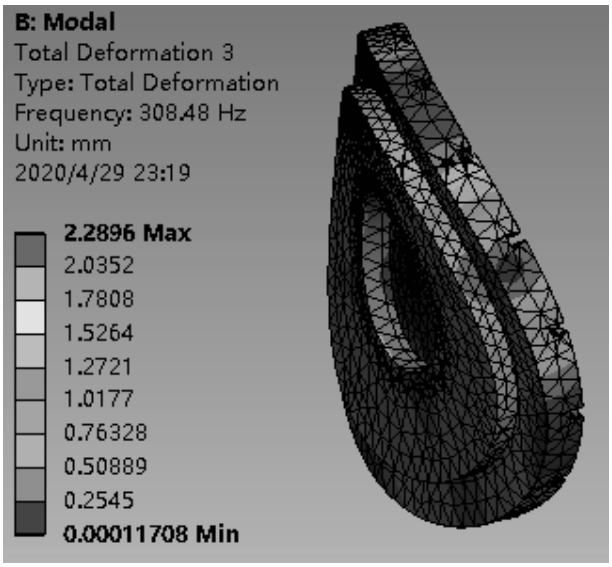

c) Third-order mode

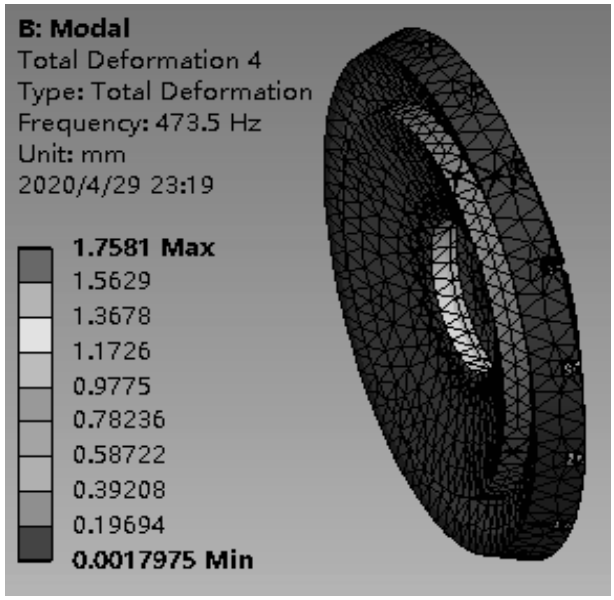

d) Fourth-order mode

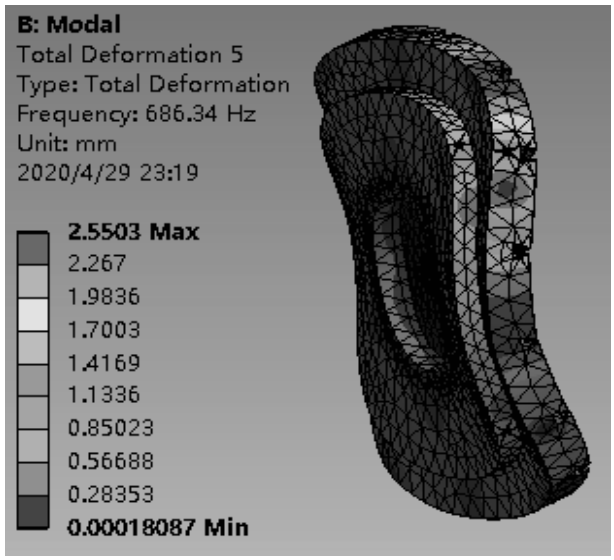

e) Fifth-order mode

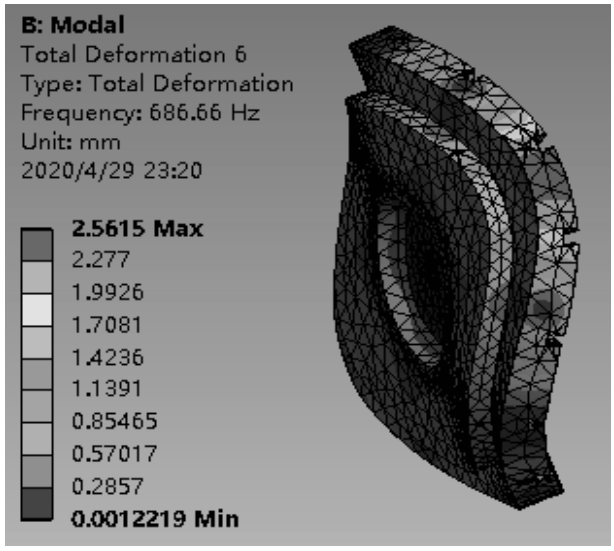

f) Sixth-order mode

Fig. 6 *The first six modes of marble (29400N).*

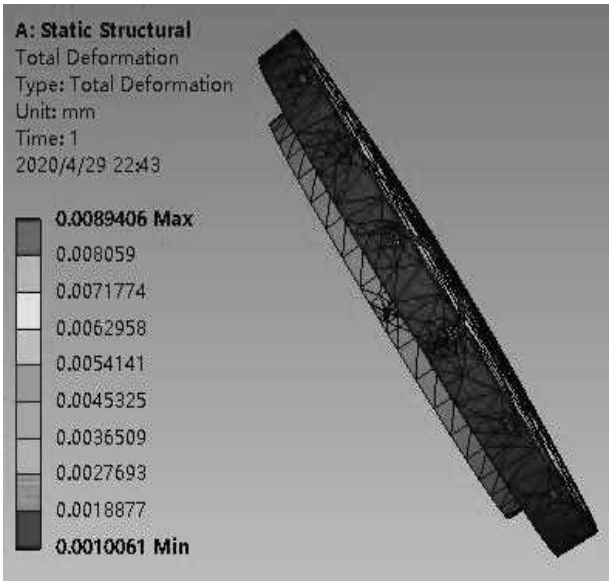

Fig. 7 *40Cr maximum displacement (29400N).*

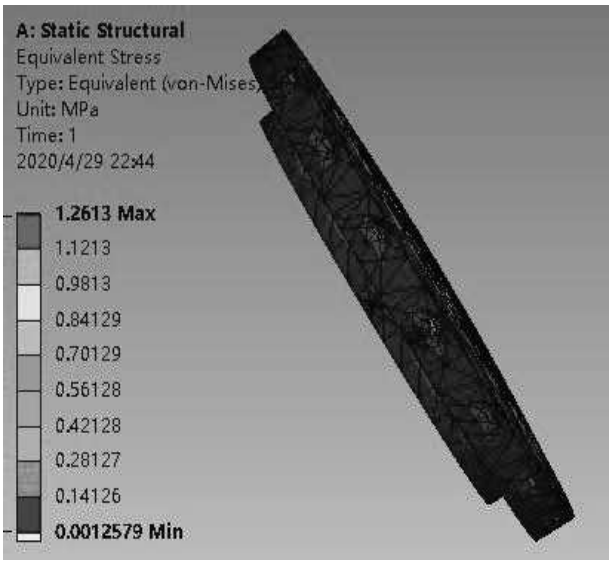

Fig. 8 *40Cr maximum stress (29400N).*

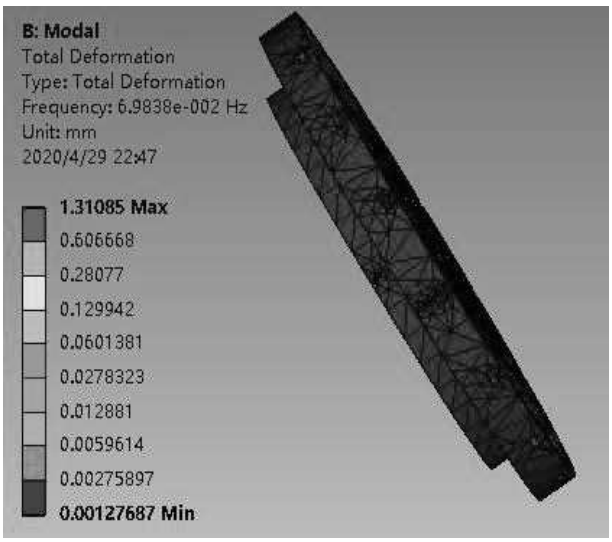

a) First-order mode

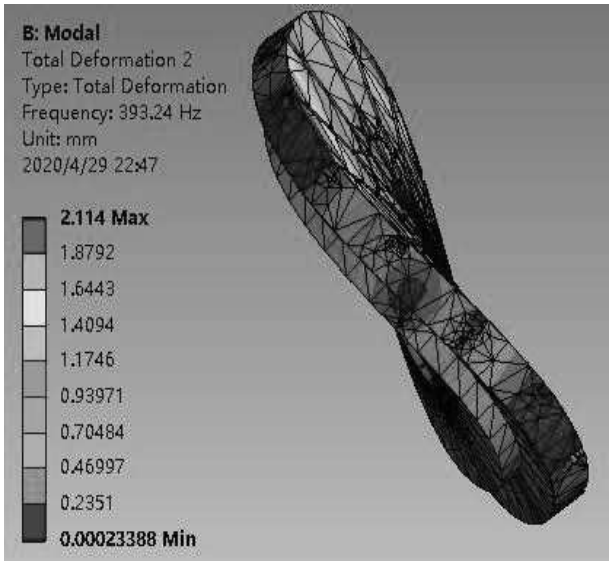

b) Second-order mode

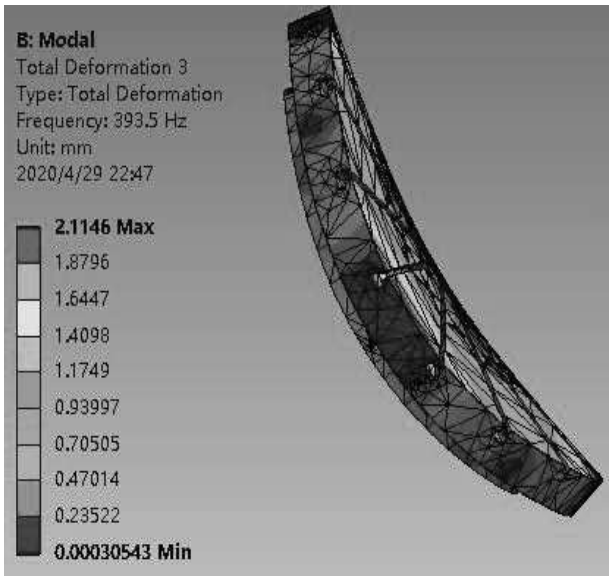

c) Third-order mode

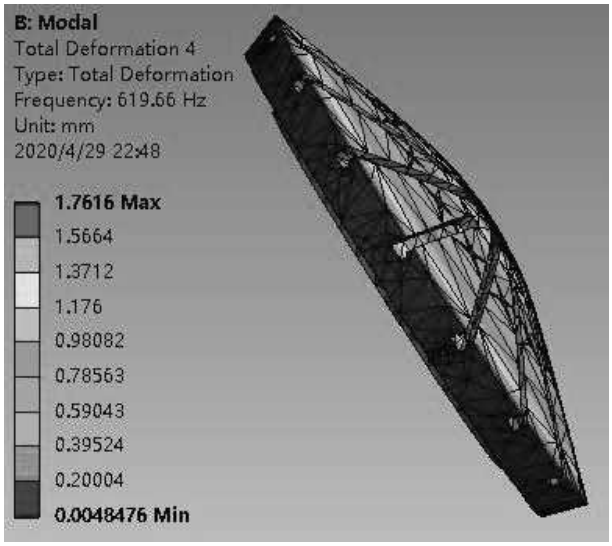

d) Fourth-order mode

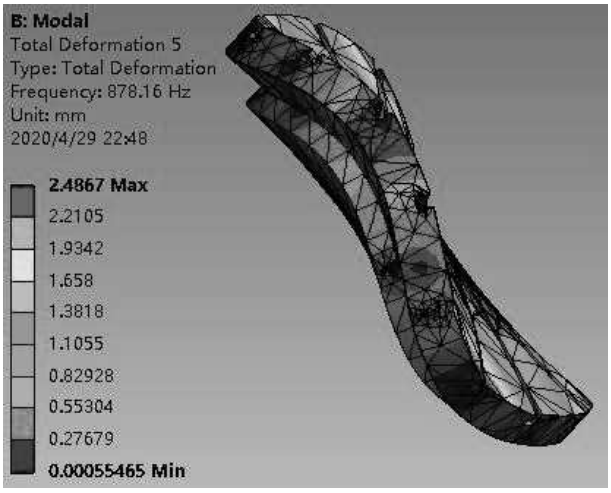

e) Fifth-order mode

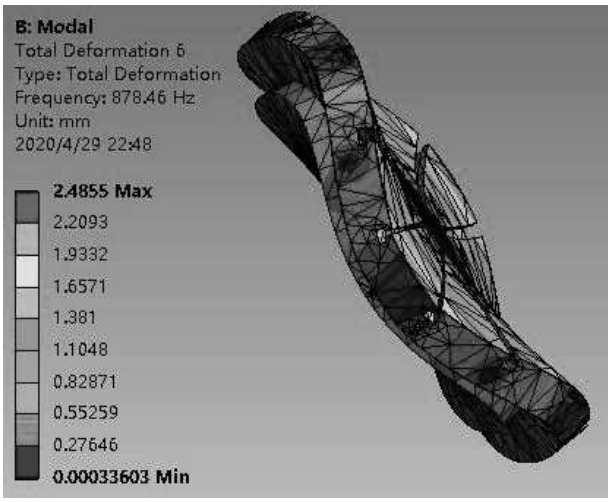

f) Sixth-order mode

Fig. 9 *The first six modes of 40Cr (29400N).*

Analyzing the data in Fig. 3 from a macro perspective, it can be concluded that although the 40Cr is about smaller than the marble in terms of the maximum displacement as a whole, the maximum displacement of 40Cr increases sharply to 8.9406 μm when reaching the applied force limit of 29400N. In contrast, the maximum displacement of marble slowly increases with the increase of force. When the limit force is 29400N, it only reaches 2.6 μm, which far meets the processing requirements. Meanwhile, according to the analysis of power consumption equation $P=\frac{T}{9550\cdot n}=\frac{F\cdot r}{9550\cdot n}=\frac{m\pi nd\cdot r}{9550\cdot n}$. The power consumption increases with the increase of mass m. According to the density lesson in Table 1, the power consumed by marble is reduced by 39.12% compared with 40Cr. From the aspects of weight and material saving of hydrostatic turntable, the weight of marble is reduced by 39.36% compared with 40Cr. According to the analysis of Figs. 5 and 8, the maximum stress of both is small. However, according to the analysis of the first mode shapes of the two materials in Figs. 6 and 9, it is shown that marble is about 21.59% higher than 40Cr. Among them, the most important factor is that 40Cr will appear oxidation and other inevitable factors with the increase of machine tools service life. It will inevitably lead to a sharp drop in machining accuracy. Marble avoids this bad factor.

4 Test processing

Based on the above analyzed results, processing, manufacturing and assembly are performed, as shown in Fig. 10.

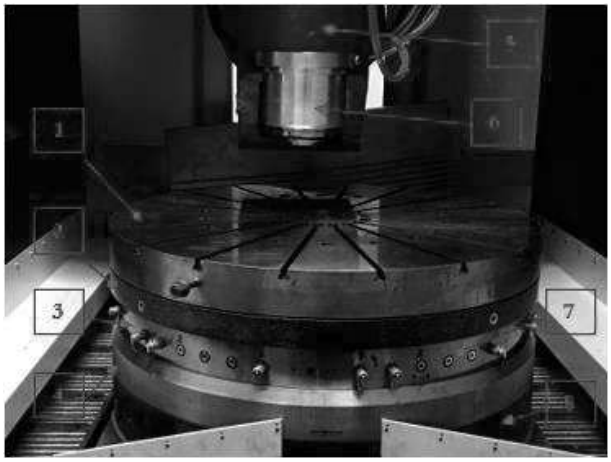

1 40Cr table top; 2 marble turntable; 3 bearing bush; 4 seal oil ring; 5 45° swing head; 6 TDM motorized spindle; 7 oil pressure regulating hole; 8 foundation bed

Fig. 10 *Field assembly drawing of hydrostatic turntable.*

As shown in Fig. 10, the uppermost table surface 1 of the hydrostatic turntable is made of 40Cr and clamps the workpiece in direct contact with the tool mounted on the motorized spindle 6. However, the lower surface of the marble turntable 2 is in direct contact with the oil in the hydrostatic turntable to ensure the rotation accuracy of the hydrostatic turntable. With the increase of the service life of the machine tool, the marble turntable in direct contact with the oil will give full play to its advantages and still maintain high support and rotation accuracy.

5 Conclusion

(1) This paper mainly studied the structural innovation of hydrostatic turntable in high precision machining equipment for aerospace parts. It is proposed to replace the traditional 40Cr with marble and appled it to the components of the hydrostatic turntable. The vibration mathematical model of the components is analyzed, and the differences between the two materials are compared through software simulation.

(2) From the analyzed results, it is found that marble is better than 40Cr for some parts of hydrostatic

turntable in high precision equipment. From the analysis of the maximum displacement, when reaching the applied force limit of 29400N, the maximum displacement of 40Cr increases sharply to 8.9406μm; While the marble reaches 2.6μm. In particular, it is analyzed that the power consumed by marble is reduced by 39.12% compared with 40Cr. The weight of marble is reduced by 39.36% compared with 40Cr. In terms of vibration mode, marble is about 21.59% higher than 40Cr. At the same time, it is inferred from the analysis of all the data that with the increase of the service life of this ultra-precision equipment, the machine tools made of marble for some parts is better than the machine tools made of 40Cr in terms of overall accuracy retention and processing accuracy stability of related parts. Therefore, through the above analysis and recommendation, the actual processing is carried out, and the hydrostatic turntable is assembled to process high-precision aerospace parts.

Acknowledgment

This research was funded by [National Key Research and Development Program of China] grant number [2018YFB2000502] and [National Science and Technology Major Project of the Ministry of Science and Technology of China] grant number [2018ZX04002001] and [National Science and Technology Major Project] grant number [2017-VII-0001-0094].
The authors declare no conflicts of interest.

References

[1] CHRISTIAN BRECHER, P UTSCH, R KLAR, (2010). *Christian Wenzel. Compact design for high precision machine tools*, pp. 50(4): 328-334. *International Journal of Machine Tools & Manufacture*.

[2] CHEN, EN PING, LI, SHAO HUI, WU, FENG HE. (2014). Structure Design of Biaxial Rotary Milling Head with High-Torque, High-Precision and Mechanical Spindle, pp. 621:337-345.*Key Engineering Materials*.

[3] CHEN, WANQUN, LUO, XICHUN, SU, HAO. (2016). An integrated system for ultra-precision machine tool design in conceptual and fundamental design stage, pp. 84(5-8):1177-1183. *International Journal of Advanced Manufacturing Technology*.

[4] YINGCHUN LIANG, WANQUN CHEN, YANG SUN, GUODA CHEN. (2012). Dynamic design approach of an ultra-precision machine tool used for optical parts machining, pp. 226(11):1930-1936. *Proceedings of the Institution of Mechanical Engineers Part B Journal of Engineering Manufacture*.

[5] GUODA CHEN, YAZHOU SUN, FEIHU ZHANG. (2018). Dynamic Accuracy Design Method of Ultra-precision Machine Tool, pp. 031(002):158-166. *Chinese Journal of Mechanical Engineering*.

[6] YONGSHENG ZHAO, HONGCHAO WU, CCONGBIN YANG. (2019). Effect of guide rail profile errors on the motion accuracy for a heavy-duty hydrostatic turntable, pp. 233(15). *Archive Proceedings of the Institution of Mechanical Engineers Part C Journal of Mechanical Engineering Science*.

[7] ZHAOMIAO LIUI, CHENGYIN ZHANG, FENG SHEN. (2011). Influence of boundary conditions and turntable speeds on the stability of hydrostatic oil cavity, pp. 6(3):359-368. *Frontiers of Mechanical Engineering*.

[8] IWASAKI MAKOTO, MIYAJI MASASHI, MATSUI NOBUYUKI. (2005). High-Precision Contouring Control of Table Drive System in Machine Tools Using Lost Motion Compensation, pp. 125. *Ieej Transactions on Industry Applications*.

[9] YU ADONG, WANG PINGJUN, LI XIANGLONG. (2016). Research on New Turntable Technology for Improving Large and High Precision Vertical Machine Tool Accuracy Retention, pp. 14. *Machine Tool & Hydraulics*.

[10] FU ZHIFANG, (1990). *Vibration Modal Analysis and Parameter Identification*. Beijing: Beijing Machinery Industry Press.

[11] ZHANG HUA, ZHAO LEI, CHEN HUA (2019). Research on Hydraulic System Optimization of Loader Based on GA-BP, pp. 19(6):952-958. *Manufacturing Technology*.

[12] MÁRIA BLATNICKÁ, MIROSLAV BLATNICKÝ, JÁN DIŽO, MILAN SÁGA. (2018). Comparison of Analytical Stress Analysis and Numerical Calculation of Mobile Work Machine Part, pp. 18(2):190-193. *Manufacturing Technology*.

[13] LIU CHENGPEI, HU JUNPING. (2018). A FSI-thermal model to analyze performance characteristics of hydrostatic turntable, pp. 70(9):1692-1698. *Industrial Lubrication & Tribology*.